

Strain dependence of thermal conductivity of [0001]-oriented GaN nanowires

Kwangsub Jung,¹ Maenghyo Cho,¹ and Min Zhou^{1,2,a)}

¹*School of Mechanical and Aerospace Engineering, Seoul National University, Seoul 151-742, Republic of Korea*

²*George W. Woodruff School of Mechanical Engineering, Georgia Institute of Technology, Atlanta, Georgia 30332, USA*

(Received 16 September 2010; accepted 8 January 2011; published online 28 January 2011)

The thermomechanical behavior of [0001]-oriented GaN nanowires with 2.26 and 3.55 nm in diameter under tensile loading is analyzed using molecular dynamics simulations with the Green–Kubo method and quantum correction. A phase transformation from wurtzite to a tetragonal structure is observed. The thermal conductivity is found to decrease as the wires undergo tensile deformation and phase transformation, except for the smallest diameter and temperatures above 1495 K at which it remains largely constant as the axial strain increases. The different trends appear to result from phonon behavior changes primarily associated with the surface structures of the nanowires at the different conditions. © 2011 American Institute of Physics.

[doi:10.1063/1.3549691]

The coupling between the thermal and mechanical behaviors of nanostructures is important because it provides a mechanism for designing nanoscale devices and for enhancing the performance of devices. The variation with loading or deformation of thermal conductivity of nanowires and nanofilms of a range of materials is of particular interest and has been extensively studied.^{1–6} For example, it has been reported that a structural transformation from wurtzite (WZ) to a graphitelike (HX) structure in [011̄0]-oriented ZnO nanowires under tensile loading causes significant changes in the thermal conductivity of the nanowires.^{2,7} The dominant effects that cause the conductivity change come from differences in density of the crystalline structures.

In related studies, a tetragonal structure (TS) with four-atom rings is observed in [0001]-oriented ZnO (Refs. 8 and 9) and GaN (Ref. 10) nanowires. This structure results from a phase transformation from WZ under uniaxial tensile loading. So far, thermal response changes of the nanowires associated with this structural transform have not been studied. Here, we report the results of molecular dynamics (MD) calculations that relate to the response changes. The focus is on the thermal conductivity of wires of different sizes at different temperatures. To obtain a more accurate quantification of the conductivity and temperature, the empirical approach of Lee *et al.*¹¹ for quantum correction of MD data and temperature is used.

In this analysis, GaN nanowires with the WZ structure and a hexagonal cross section like that in Fig. 1 of Ref. 10 are considered. The axis of the nanowires is in the [0001] crystalline direction. Periodic boundary conditions are specified in the axial direction and the lateral surfaces of the wires are traction-free. The length of the wires is 14.45 nm and the diameters considered are 2.26 and 3.55 nm. The calculations are carried out using the LAMMPS code.¹² The Buckingham potential¹³ is used to describe the short range interactions between atoms and the Wolf summation^{14,15} is used to evalu-

ate the long-range Coulombic forces. This potential reproduces the structural, elastic, and dielectric constants of the WZ, zinc-blende, and rocksalt structures.¹³ Native-defect formation and surface relaxation are also effectively predicted.¹³ The results obtained by using this potential are quite consistent with data obtained from density functional theory calculations.⁸ In particular, this potential correctly predicts the WZ-to-TS transformation. In contrast, the Stillinger–Weber potential and the Tersoff potential do not predict these transformations of GaN. The wires are equilibrated for 100 ps by using a one-direction NPT algorithm before the thermomechanical analysis. Tensile deformation is carried out at a strain rate of 0.05 ns⁻¹. The Green–Kubo method for equilibrium MD calculations¹⁶ is used and the heat flux at each strain is calculated over period of 8 ns in NVE ensemble. Thermal conductivity in the wire axis direction is calculated using the heat current autocorrelation function. The thermal conductivity values reported are averages of three simulations which are different only in initial random realization of atomic velocities.

The thermal conductivity and temperature calculated from MD simulations, especially at temperatures below the Debye temperature, are only approximate because quantum effects are neglected. Quantum corrections¹¹ are applied to both quantities. The quantum-corrected thermal conductivity is

$$\kappa_Q = \kappa_{MD} \frac{dT_{MD}}{dT_Q}, \quad (1)$$

where κ_{MD} is the conductivity from MD calculations and the scaling factor dT_{MD}/dT_Q is obtained by dividing the heat capacity from first-principles calculations¹⁷ by that from MD, i.e.,

$$\frac{dT_{MD}}{dT_Q} \approx \frac{C_V(T)}{3Nk_B}. \quad (2)$$

Here, $C_V(T)$ is a function of temperature T , N is the number of atoms in the system, and k_B is the Boltzmann constant. $C_V(T)$ is close to zero near 0 K and increases with tempera-

^{a)}Electronic mail: min.zhou@gatech.edu. Tel.: 404-894-3294. FAX: 404-894-0186.

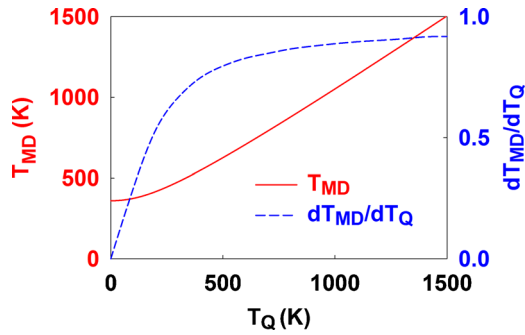


FIG. 1. (Color online) MD temperature (T_{MD}) and the scaling factor dT_{MD}/dT_Q as functions of quantum temperature (T_Q).

ture, converging to the MD value of $3Nk_B$ at temperatures well above the Debye temperature (≈ 800 K for GaN). The scaling factor dT_{MD}/dT_Q increases from 0 and approaches 1 as temperature increases from 0 K to above the Debye temperature. The mapping from the temperature calculated using MD (T_{MD}) to the quantum-corrected temperature (T_Q) and the scaling factor defined in Eq. (2) are given in Fig. 1. When $T_{MD}=500$ K, the corresponding quantum temperature is $T_Q=334$ K and scaling factor is 0.697. In contrast, when $T_{MD}=1500$ K, $T_Q=1495$ K and the scaling factor is 0.918. The heat capacity of WZ GaN is used in evaluating the scaling factor for TS GaN because changes in heat capacity during the phase transformation are negligible.^{18–20}

Figure 2 shows the thermal conductivity and stress²¹ as functions of strain for a nanowire with diameter $d=2.26$ nm at $T_Q=334$ K ($T_{MD}=500$ K). When the strain reaches 0.06, the stress drops precipitously. This drop is associated with the phase transformation from the WZ structure to the TS structure similar to that reported for ZnO by Wang *et al.*⁸ After the completion of the transformation, the wire deforms elastically in the TS structure (as indicated by the steady increase in stress following the precipitous drop) and eventually breaks into two pieces at a strain of 0.17 (as indicated by the second precipitous drop in stress). The phase transformation is also observed for strain rates as low as 0.005 ns⁻¹.

The mechanical deformation and structural change induce changes in the thermal response of the nanowire as well. The thermal conductivity decreases from its initial value of 12.5 W/mK by 45% as the strain increases to 0.15. Overall, the decrease is gradual and steady. Thermal conductivity does not show a significant or abrupt change during the

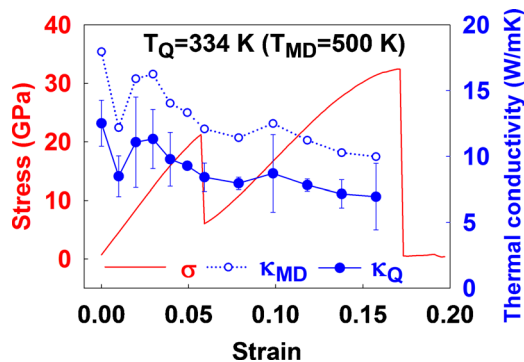


FIG. 2. (Color online) Stress and uncorrected MD and quantum-corrected thermal conductivities as functions of strain for a nanowire with diameter $d=2.26$ nm at 334 K. Error bars denote standard deviation of conductivity.

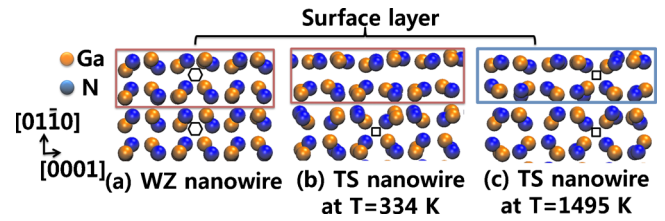


FIG. 3. (Color online) Arrangement of atoms in the interior and on the surfaces of a nanowire with $d=2.26$ nm: (a) WZ-structured wire at zero strain; (b) TS-structured wire at strains of 0.08 and 334 K, this wire has a surface layer whose structure is very different from that in the interior; and (c) TS-structured wire at strains of 0.08 and 1495 K, this wire has the same structure on the surface and in the interior.

onset, progression, and completion of the WZ-to-TS transformation, although the stiffness of the nanowire decreases by 21% (394–310 GPa) and the phonon group velocity, which is related to thermal conductivity,²² decreases by 12%. The phonon group velocity may not be the dominant factor affecting the conductivity of semiconducting nanowires.² For $[01\bar{1}0]$ -oriented ZnO nanowires, the conductivity shows a significant change during the WZ-to-HX transformation, as shown in Fig. 1 of Ref. 2. The conductivity decreases as the strain increases before the transformation but begins to increase when the fraction of HX exceeds that of WZ. Dominant effects that cause the conductivity of the HX-structured wires to be higher than that of the WZ-structured wires come from the higher density of HX than that of WZ. The efficient packing of the HX structure and its higher density lead to a lower anharmonicity in lattices and in turn the higher thermal conductivity. However, the density of the TS structure reported here is almost the same as that of WZ. This results in a different trend in conductivity during the WZ-to-TS transformation from that during the WZ-to-HX transformation. The result is very little change in conductivity during the WZ-to-TS transformation in terms of bulk contribution.

On the other hand, the differences in surface configurations between the two cases contribute to the change in conductivity. As shown in Fig. 5 of Ref. 2, the atomic arrangement on the surfaces of the WZ-structured ZnO wires shows surface reconstruction, but the atomic arrangement of HX-structured ZnO wires is similar to that in the core. The surface disorder is significantly lower for HX-structured wires than that of WZ-structured wires. This difference significantly increases the conductivity of $[01\bar{1}0]$ -oriented wires during the WZ-to-HX transformation. Because the surface of the TS-structured wires in Fig. 3(b) has a higher disorder than that of the WZ-structured wires in Fig. 3(a), surface scatter of phonons is more pronounced for the TS-structured wires, causing the conductivity to be lower.^{23,24}

The mechanical and thermal behaviors of the same nanowire at $T=1495$ K (54% of the melting point of GaN) are also analyzed. As shown in Fig. 4, the stress-strain curve shows a similar trend as that for $T=334$ K in Fig. 2, indicating that the overall mechanical response and structure transformation are essentially the same. However, the thermal conductivity remains essentially constant for strains up to 0.12. This is in contrast to what is seen for the lower temperature case in Fig. 2. The different trends at the low and high temperatures come primarily from the different atomic arrangements on the wires' surfaces in the two cases. The atomic arrangement on the surfaces of the unstrained

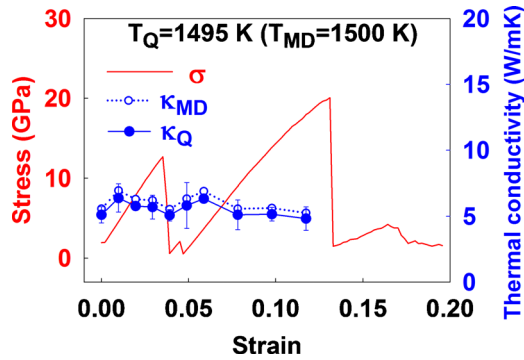


FIG. 4. (Color online) Stress and uncorrected MD and quantum-corrected thermal conductivities as functions of strain for a nanowire with diameter $d=2.26$ nm at 1495 K. Error bars denote standard deviation of conductivity.

wire is similar to that in the interior of the wire, as shown in Fig. 3(a). The surface structure of the stretched wire varies with temperature. At 334 K, the structure on the surfaces is different from the TS structure in the interior, as shown in Fig. 3(b). At 1495 K, the atomic arrangement on the surfaces of the stretched wire is similar to that in the interior, as shown in Fig. 3(c). Moreover, the atomic alignment along the [0001] direction of TS-structured wire is similar to that of the initial WZ-structured wire. Consequently, the conductivity remains essentially constant as strain increases and the structure transformation occurs at this temperature. The decrease in conductivity at 334 K is mainly due to the surface reconstruction induced by the tensile deformation.

Figure 5 shows the dependence of thermal conductivity on temperature for bulk WZ GaN and wires 2.26 and 3.55 nm in diameter. Over the range of 334–1495 K, the conductivity values at two typical strain levels decrease as temperature increases. At 1495 K, the conductivity of the wire with $d=3.55$ nm decreases 33% as strain increases from 0.0 to 0.08. The conductivity of bulk WZ GaN reflects the effect of phonon-phonon scattering without the influence of surfaces.²⁵ The contribution of the surface scattering to the conductivity of the wires is dominant but decreases with temperature. When temperature increases from 334 to 1495 K, the conductivity of bulk decreases by 74%. In contrast, the conductivity of the wires decreases by 59% ($d=2.26$ nm) and 43% ($d=3.55$ nm). The phonon mean free

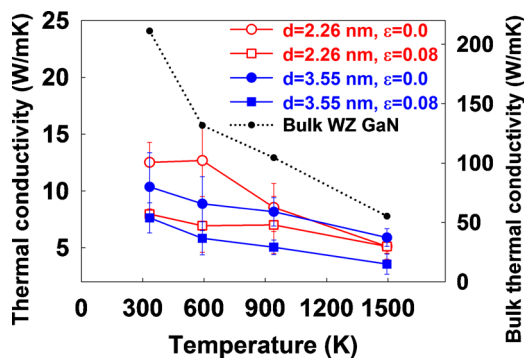


FIG. 5. (Color online) Thermal conductivity as a function of temperature for bulk WZ GaN and nanowires with diameters of 2.26 and 3.55 nm at strains of 0.0 and 0.08. Error bars denote standard deviation.

paths for bulk GaN are approximately 50 nm at 334 K and 10 nm at 1495 K, much larger than the diameter of the wires considered. We note that the conductivity of the wire with $d=3.55$ nm is lower than that of the wire with $d=2.26$ nm at temperatures between 334 and 941 K. The results are within the error bars of the respective curves, indicating that the conductivity does not change significantly between these two sizes over the temperature range and that the surface effect dominates.

In summary, the thermal conductivity of [0001]-oriented GaN nanowires under uniaxial tensile loading is analyzed. Overall, the conductivity decreases as strain increases primarily due to the formation of a surface layer. One exception is the nanowire with the small diameter of $d=2.26$ nm at temperatures above $T=1495$ K. In such cases, the wire does not show a surface layer and the atomic arrangements on the surface and in the interior are similar. As a result, the thermal conductivity remains essentially constant as strain increases, even after a phase transformation occurs. Another contributing factor is that the atomic alignments in the [0001] wire axial direction for the original wurtzite structure and resulting tetragonal structure are similar.

Support by the NRF of Korea through the NRL (Grant No. 2010-0018920) and WCU (Grant No. R31-2009-000-10083-0) with funding from the MEST is acknowledged.

- ¹R. C. Picu, T. Borca-Tasciuc, and M. C. Pavel, *J. Appl. Phys.* **93**, 3535 (2003).
- ²A. J. Kulkarni and M. Zhou, *Nanotechnology* **18**, 435706 (2007).
- ³Y. Xu and G. Li, *J. Appl. Phys.* **106**, 114302 (2009).
- ⁴X. Li, K. Maute, M. L. Dunn, and R. Yang, *Phys. Rev. B* **81**, 245318 (2010).
- ⁵J. Liu and R. Yang, *Phys. Rev. B* **81**, 174122 (2010).
- ⁶C. Ren, W. Zhang, Z. Xu, Z. Zhu, and P. Huai, *J. Phys. Chem. C* **114**, 5786 (2010).
- ⁷A. J. Kulkarni and M. Zhou, *Appl. Phys. Lett.* **88**, 141921 (2006).
- ⁸J. Wang, A. J. Kulkarni, K. Sarasamak, S. Limpijumnonng, F. J. Ke, and M. Zhou, *Phys. Rev. B* **76**, 172103 (2007).
- ⁹J. Wang, A. J. Kulkarni, F. J. Ke, Y. L. Bai, and M. Zhou, *Comput. Methods Appl. Mech. Eng.* **197**, 3182 (2008).
- ¹⁰P. Xiao, W. Wang, J. Wang, F. Ke, M. Zhou, and Y. Bai, *Appl. Phys. Lett.* **95**, 211907 (2009).
- ¹¹Y. H. Lee, R. Biswas, C. M. Soukoulis, C. Z. Wang, C. T. Chan, and K. M. Ho, *Phys. Rev. B* **43**, 6573 (1991).
- ¹²S. J. Plimpton, *J. Comput. Phys.* **117**, 1 (1995).
- ¹³P. Zapol, R. Pandey, and J. D. Gale, *J. Phys.: Condens. Matter* **9**, 9517 (1997).
- ¹⁴D. Wolf, P. Keblinski, S. R. Phillpot, and J. Eggebrecht, *J. Chem. Phys.* **110**, 8254 (1999).
- ¹⁵C. J. Fennell and J. D. Gezelter, *J. Chem. Phys.* **124**, 234104 (2006).
- ¹⁶S. G. Volz and G. Chen, *Phys. Rev. B* **61**, 2651 (2000).
- ¹⁷H. Y. Wang, H. Xu, T. T. Wang, and C. S. Deng, *Eur. Phys. J. B* **62**, 39 (2008).
- ¹⁸J. S. Kurtz, R. R. Johnson, M. Tian, N. Kumar, Z. Ma, S. Xu, and M. H. W. Chan, *Phys. Rev. Lett.* **98**, 247001 (2007).
- ¹⁹A. Seko, F. Oba, A. Kuwabara, and I. Tanaka, *Phys. Rev. B* **72**, 024107 (2005).
- ²⁰H. Y. Wu, X. L. Cheng, C. H. Hu, and P. Zhou, *Physica B* **405**, 606 (2010).
- ²¹M. Zhou, *Proc. R. Soc. London, Ser. A* **459**, 2347 (2003).
- ²²M. C. Roufosse and R. Jeanloz, *J. Geophys. Res.* **88**, 7399 (1983).
- ²³L. Shi, Q. Hao, C. Yu, N. Mingo, X. Kong, and Z. L. Wang, *Appl. Phys. Lett.* **84**, 2638 (2004).
- ²⁴A. L. Moore, M. T. Pettes, F. Zhou, and L. Shi, *J. Appl. Phys.* **106**, 034310 (2009).
- ²⁵J. Zou, *J. Appl. Phys.* **108**, 034324 (2010).